Integrated Operation of Droop Controlled Electrical Networks with District Heating Networks

Styliani A. Vomva
Dept. of Electr. & Comput. Eng.
Aristotle University of Thessaloniki
Thessaloniki, Greece
stylianav@ece.auth.gr

Georgios C. Kryonidis
Dept. of Electr. & Comput. Eng.
Aristotle University of Thessaloniki
Thessaloniki, Greece
kryonidi@ece.auth.gr

Angelos I. Nousdilis
Dept. of Electr. & Comput. Eng.
University of Western Macedonia
Koila, Greece
a.nousdilis@uowm.gr

Georgios C. Christoforidis
Dept. of Electr. & Comput. Eng.
University of Western Macedonia
Koila, Greece
gchristoforidis@uowm.gr

Grigoris K. Papagiannis
Dept. of Electr. & Comput. Eng.
Aristotle University of Thessaloniki
Thessaloniki, Greece
gpapagia@ece.auth.gr

***Abstract*—Nowadays, there is a growing need to increase the penetration of distributed renewable energy sources (DRESs) in electrical distribution grids in an attempt to decarbonize the energy sector. Nevertheless, the intermittent nature of DRESs introduces several challenges towards the secure and reliable operation of distribution grids, and especially of low-voltage (LV) grids, such as overvoltages. In this work, the integrated operation of electrical distribution grids equipped with droop control schemes for DRES and district heating systems is proposed to tackle this issue. It is concluded that the integrated operation can act as a means towards overvoltage mitigation, while ensuring reduced network losses and active power curtailment, thus better exploiting the DRES potential.**

***Index Terms*—Active power control, district heating network, electrical network, integrated operation, reactive power control, voltage regulation.**

I. Introduction

Worldwide, several initiatives have been launched both at national and international levels to tackle climate change by minimizing greenhouse gas emissions. According to the recently revised directive [1], European Union has set a target of 32 % of renewable energy sources (RES) share in the gross final energy consumption in 2030. In this framework, the further installation of distributed RES (DRES) in the existing electrical networks (ENs) is rapidly evolving, with the photovoltaic (PV) systems being mostly preferred because of their modular structure and their advanced technology.

However, the further penetration of DRES into the existing systems may lead to technical challenges related to their intermittent nature, which results in unbalances between supply and demand. This can affect the reliable operation of the ENs in cases of high DRES penetration [2]. The most common issue is to maintain the network voltages within the permissible limits. Considering low-voltage (LV) distribution grids, these limits are 0.9 and 1.1 p.u. [3]. Regarding the voltage regulation of ENs with high DRES penetration, several solutions have been proposed in the literature that can be classified into two main categories, i.e., the active power control (APC) [4] and the reactive power control (RPC) [5] schemes. Another promising solution is to add more flexibility to ENs by connecting other energy systems [6], thus forming the well-established multi-energy systems (MESs) [7].

The integration of energy systems has been envisioned by the European Commission [8], which also proposed a set of actions in this direction [9]. Among the different systems that can be integrated, the combined operation of ENs and district heating networks (DHNs) has gained great attention. From a technical point of view, the coupling of ENs and DHNs is mainly based on the electrification of the thermal loads, which can lead to improved exploitation of the DRES generation and to the decrease of the curtailed power [10] – [12]. Integration of the EN and DHN can lead to the cost minimization of the overall system operation [13] – [16]. In fact, such an integration has been proposed instead of investing in expanding the DHNs [17]. Also, this scheme can have positive effects to the reliable operation of the ENs, as the excess energy is utilized to meet the thermal needs, preventing the reverse power flow in ENs. In this way, the potential of DHNs is untapped by providing voltage support to ENs thus mitigating potential overvoltages [18], [19]. However, the effectiveness of the integration has not been evaluated when APC or RPC schemes are applied to the DRES units connected to the EN.

In this paper, the integrated operation of EN and DHN is proposed when a droop-based APC/RPC scheme is applied to the DRES units. The performance of the control strategies under study is evaluated in terms of mitigating overvoltages, leading also to reduced network losses both in EN and in DHN and to reduced amounts of power that need to be curtailed by the DRES units to tackle overvoltages.

The remaining of the paper is organized as follows. A detailed modeling of ENs and DHNs is presented in Section II. The methodological approach for the effective integration of ENs and DHNs is described in Section III. Section IV describes the system under analysis and the corresponding results are presented in Section V. Finally, Section VI concludes the paper.

II. Theoretical background

A. Electrical Network Model

Assuming an EN with N nodes, the modeling of the EN is based on the electrical power flow equations relating the nodal active and reactive power with nodal voltages, (1) and (2), respectively. P_i, Q_i, V_i, δ_i are the active power, the reactive

Citation information, DOI: 10.1109/SyNERGYMED55767.2022.9941443

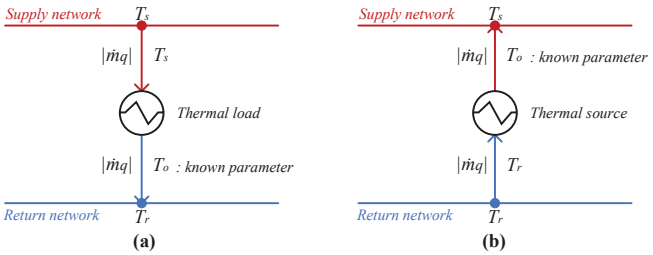

Fig. 1. Modeling of load and source in DHN, showing the actual flow of the heat medium. (a) Load and (b) source.

power, the voltage magnitude and the voltage angle at the i-th node of the system, δ_j is the voltage angle at the j-th node of the system, while y_{ij} and γ_{ij} stand for the magnitude and the angle of the admittance of the line ij, which connects node i with node j, respectively.

$$P_i = \sum_{j=1}^{N} |V_i||V_j||y_{ij}|cos(\delta_j - \delta_i + \gamma_{ij}) \quad \forall i \in N \tag{1}$$

$$Q_i = -\sum_{j=1}^{N} |V_i||V_j||y_{ij}|sin(\delta_j - \delta_i + \gamma_{ij}) \quad \forall i \in N \tag{2}$$

B. District Heating Network Model

A DHN is comprised of the following: (a) a main source acting as a slack bus, (b) nodes where the thermal loads/sources are connected to, and (c) two sets of pipes, one for the supply and one for the return subsystem [20]. The main difference between those two subsystems is the temperature level, with the return subsystem having lower temperatures than the supply subsystem. The supply and return subsystems of a DHN are connected via the loads and the sources. Distributed thermal sources can be also considered in a DHN, as an analogous of the DRESs connected to ENs. In such a case, the heat medium from the return network is inserted into the sources where its temperature is increased up to a predefined value. The reverse process is followed for the thermal loads; the heat medium from the supply network is inserted to the load where its temperature is reduced down to a certain level [21].

Based on the above analysis, it can be derived that two types of nodes in DHNs exist, i.e., nodes where (a) loads and (b) sources are connected, as depicted in Fig. 1. $\dot{m}_q$ is the nodal mass flow into a load or a source. Each load/source is associated with the following temperatures:

- T_s, which is the node temperature of the supply subsystem;
- T_r, which is the node temperature of the return subsystem;
- T_o, which is the outlet temperature of the load/source before mixing in the network. T_o is assumed to be an a priori known parameter of the system, i.e., the temperature of the heat medium flowing from the load to the return subsystem and from the source to the supply subsystem.

To achieve a generic DHN modeling, a variable mass flow and variable temperature (VF-VT) scheme is assumed [22]. This means that both the temperature along the nodes of the supply and return subsystems, and the mass flow at each one of the pipes are unknown variables. A combined hydraulic-thermal model as described in [20] is used to calculate the variables.

1) Hydraulic model: For a K-node DHN, the continuity of flow is expressed as follows:

$$\sum_{p \in I_k} \dot{m}_p - \sum_{p \in O_k} \dot{m}_p = \dot{m}_q^k \quad \forall k \in K \tag{3}$$

where $\dot{m}_p$ is the mass flow in the p-th pipe and $\dot{m}_q^k$ is the nodal mass flow into the load/source connected to the k-th node. I_k stands for the set of pipes where the flow comes into the node k and O_k is the set of pipes where the flow leaves the node k. This means that the sum of the mass flow that enters a node is equal to the sum of the mass flow that leaves the node plus the mass flow flowing into the connected load/source, assuming that this is a negative value for the case of a source node. The continuity of flow for the entire DHN is expressed through (4), where $\mathbf{A}$ denotes the network incidence matrix [20], $\dot{\mathbf{m}}$ is the vector of the mass flow into all the network pipes, and $\dot{\mathbf{m}}_\mathbf{q}$ is the vector of the nodal mass flow.

$$\mathbf{A} \cdot \dot{\mathbf{m}} = \dot{\mathbf{m}}_\mathbf{q} \tag{4}$$

Eq. (3) and (4) express the hydraulic model of a radial DHN. For meshed DHNs, additionally, the sum of pressure drops/rises in closed loops should be considered equal to zero.

2) Thermal model: Assuming that M is a subset of K where a thermal load/source is connected, (5) models the relationship between the thermal power and the temperature difference corresponding to each load/source; Φ_k expresses the thermal power of the source/load connected to the k-th node, c_p is the specific heat capacity of the heat medium, $T_{k,in}$ is the temperature inserting into the load/source, i.e., T_s and T_r for a load and a source, respectively. $T_{o,k}$ is the temperature leaving the load/source connected to the k-th node before mixing with the return and the supply subsystem for a load and a source, respectively. $T_{o,k}$ corresponds to the T_o temperature and is a known parameter.

$$\Phi_k = c_p \dot{m}_q^k (T_{k,in} - T_{o,k}) \quad \forall k \in M \tag{5}$$

For DHN with P pipes, (6) expresses the heat losses and applies to both the supply and the return subsystems. Specifically, it describes the temperature drop of the heat medium in the heating network. $T_{p,start}$ and $T_{p,end}$ are the temperatures at the beginning and the outlet of the p-th pipe, and T_a is the ambient temperature which affects the operation of the DHN. λ_p, L_p and $\dot{m}_p$ stand for the heat transfer coefficient per unit length, the length and the mass flow into the p-th pipe, respectively.

$$T_{p,end} = (T_{p,start} - T_a) \cdot e^{-\frac{\lambda_p L_p}{c_p \dot{m}_p}} + T_a \quad \forall p \in P \tag{6}$$

Finally, for each one of the K nodes, the temperature of the heat medium leaving the k-th node is the same in the beginning of all the corresponding pipes. This temperature ($T_{k,out}$) is calculated via (7), based on the mixture of the incoming flow, with the heat medium flowing into a pipe and coming into the k-th node with the outlet temperature $T_{p,end}$.

$$T_{k,out} \cdot \sum_{p \in O_k} \dot{m}_p = \sum_{p \in I_k} (\dot{m}_p \cdot T_{p,end}) \quad \forall k \in K \tag{7}$$

III. Proposed Integrated Scheme

In this paper, the integrated operation of EN and DHN is proposed for the overvoltage mitigation in the EN. In the LV EN, the well-established droop control schemes are incorporated. Specifically, the APC and RPC schemes are used for the control of DRESs and their effectiveness is assessed in the case of (a) a standalone EN and (b) an integrated EN and DHN. Except for the overvoltage in the EN, the proposed integrated method is evaluated with regards to the losses that occur in both the networks, in combined operation, and to the active power curtailment level.

Regarding the APC scheme, part of the total active power of DRES injected into the LV network is curtailed, depending on the voltage at the point of common coupling (PCC) (V_i), according to (8).

$$P_{gen,i} = \begin{cases} P_{r,i} & V_i < V_{th} \\ P_{r,i}(1 - \frac{V_i - V_{th}}{V_{max} - V_{th}}) & V_{th} < V_i < V_{max} \\ 0 & V_i > V_{max} \end{cases} \quad \forall i \in G \tag{8}$$

G is a subset of the N where DRESs are connected. $P_{gen,i}$ is the active power finally injected by the DRES connected to the i-th node, while $P_{r,i}$ stands for the rated active power of the DRES. V_i is the voltage at the PCC, V_{th} represents the voltage threshold, i.e., the voltage at the PCC that triggers the active power curtailment when reached. V_{max} stands for the maximum voltage at the PCC. This strategy is efficient in LV networks because of their resistive nature and the strong dependence between the injected active power and the node voltage [23].

The RPC scheme is mathematically expressed according to (9).

$$Q_{gen,i} = \begin{cases} Q_{r,i} & V_i < V_{min} \\ Q_{r,i}\frac{V_{th}^{l} - V_i}{V_{th}^{l} - V_{min}} & V_{min} < V_i < V_{th}^{l} \\ 0 & V_{th}^{l} < V_i < V_{th}^{up} \\ -Q_{r,i}\frac{V_i - V_{th}^{up}}{V_{max} - V_{th}^{up}} & V_{th}^{up} < V_i < V_{max} \\ -Q_{r,i} & V_i > V_{max} \end{cases} \quad \forall i \in G \tag{9}$$

Here, $Q_{gen,i}$ is the output reactive power of the DRES located at i-th node, where a negative value indicates reactive power absorption. Furthermore, $Q_{r,i}$ is the corresponding rated power. V_{th}^{l} and V_{th}^{up} stand for the lower and upper voltage thresholds for the activation of the reactive power injection and absorption, respectively. V_{min} and V_{max} stand for the minimum and the maximum permissible voltage at the PCC, respectively. The RPC method consists a less efficient solution for the LV networks due to the high R/X line ratio [23].

The integrated operation of EN and DHN is achieved through coupling devices, such as heat pumps (HPs), electric boilers and combined heat and power units. In this work, HPs are assumed as the main coupling device type, operating with an unidirectional power flow, i.e., they consume electrical power from the EN to generate thermal power and provide it to the DHN. The relation between the input and the output of a HP is expressed in (10), where P_{hp}^{el} is the input electrical power, Φ_{hp} is the corresponding thermal power generated by the HP and COP denotes the coefficient of performance of the HP. It is worth mentioning that the HP is modeled as a constant power load for the electrical power simulations.

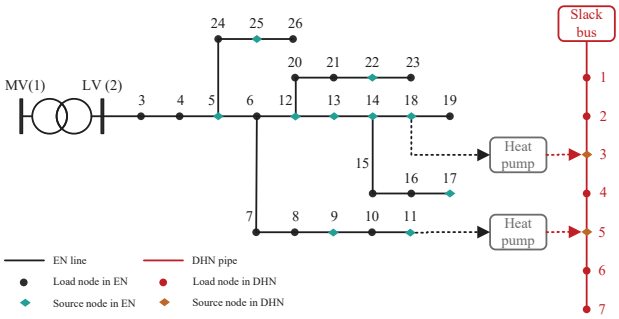

Fig. 2. Topology of the integrated electricity and district heating system.

$$P_{hp}^{el} = \Phi_{hp}/COP \tag{10}$$

In the proposed technique, the active and reactive power of the DRESs are calculated using (8) and (9), respectively. The results are considered in (1) and (2), respectively, for the nodes where the DRESs are connected. Additionally, the result from (10) is also considered in (1) for the nodes of the EN where the HPs are connected, thus leading to a corresponding increase of the electrical load. The combined analysis is achieved by solving (1) – (7), using (8) – (10).

IV. Case Study

For the evaluation of the integrated operation of EN and DHN when droop-based APC/RPC scheme is implemented, four different control strategies are studied, i.e., (a) standalone EN with an APC scheme applied to the DRES units (Strategy 1), (b) standalone EN with a RPC scheme applied to the DRESs units (Strategy 2), (c) integrated operation of EN and DHN when an APC scheme is applied to the DRES units (Strategy 3), and (d) integrated operation of EN and DHN when a RPC scheme is applied to the DRES units (Strategy 4). EN and DHN are coupled using HPs.

The performance of the proposed techniques is investigated in the integrated EN and DHN system depicted in Fig. 2. The EN comprises a small-scale LV distribution grid with high penetration of PV units. It is connected to the medium voltage (MV) grid via a 20/0.4 kV transformer. Details regarding the loads and the PV units, as well as the line characteristics are presented in [4]. A modified version of the network topology described in [4] is used, where Node 20 is connected to Node 12 instead of Node 6. The rated power factor of the PV units is equal to 0.85 in the RPC scheme. Furthermore, the voltage of the slack bus of the EN (Node 1) is equal to 1.05 p.u.. Considering the APC scheme, V_{th} and V_{max} are equal to 1.075 p.u. and 1.1 p.u., respectively. Finally, in the RPC scheme, V_{min}, V_{th}^{l}, V_{th}^{up} and V_{max} are equal to 0.9 p.u., 0.92 p.u., 1.08 p.u. and 1.1 p.u., respectively.

The DHN consists of 7 nodes. Node 1 is connected to the slack bus, i.e., a thermal-hydraulic analogous to the slack bus in ENs. This node is responsible for covering any needs that cannot be met locally, including also the thermal losses along the pipes. In this DHN, distributed thermal sources are considered transforming it into an active DHN. Thus, part of the thermal load, where these sources are connected, is covered locally, and excess energy, if any, is injected to the DHN, increasing the temperature at the connection point

TABLE I
RATED THERMAL POWER CONSUMPTION

Thermal Load	Node 2	Node 4	Node 6	Node 7
kW_{th}	40	40	30	30

TABLE II
LINE LENGTHS OF THE DHN

Line	1-2	2-3	3-4	4-5	5-6	6-7
Length (m)	400	400	600	600	600	600

TABLE III
LOSSES IN THE EN

Strategy 1	Strategy 2	Strategy 3	Strategy 4
2.6598 kW_{el}	33.1332 kW_{el}	2.4599 kW_{el}	18.1166 kW_{el}

with DHN. In this network, the outlet temperature T_o of the loads/sources is considered to be known and equal to 55 °C and 30 °C for the source and the load, respectively. The ambient temperature T_a is assumed equal to 10 °C. The temperature in both the supply and the return subsystems corresponds to the one used in the fifth generation district heating networks [24], where the heat medium temperature is low in the network pipes and distributed thermal sources are used to increase the temperature up to the desired levels.

The rated power of the thermal loads is presented in Table I, while in the source nodes, the same HP [25] is connected with rated thermal power equal to 47 kW_{th} and a COP equal to 3.16. The HPs that act as thermal sources for the DHN, behave as electrical loads in the EN, connected to the Node 11 and Node 18, respectively. For the DHN, the heat transfer coefficient λ of each pipe is considered equal to 0.2 W_{th}/mK. Water is assumed to be used as heat medium, with specific heat c_p equal to 4182 J/kgK. The line lengths of the DHN are provided in Table II.

The models of the EN and the DHN have been developed in MATLAB [26]. The power flow simulation of both the EN alone and the combined operation is implemented using FSOLVE, which comprises a non-linear equation solver.

V. RESULTS

The combined operation of EN and DHN is evaluated in terms of overvoltage mitigation. Additionally, the four control strategies described in Section IV are also compared regarding network losses and the total curtailed PV power. It is pointed out that the Strategy 0 refers to the operation of the EN without the use of any control scheme.

In Fig., 3 the voltage profile of the EN is depicted for the Strategies 0, 1 and 3. It can be seen that applying APC is efficient in mitigating the overvoltage problem, due to the resistive nature of the LV grids. In Strategy 3, the voltage is further reduced. Regarding the losses in the EN, a reduction can be observed from 2.6598 kW_{el} to 2.4599 kW_{el} when moving from Strategy 1 to Strategy 3, as can be seen in Table III. At the same time, in the Strategy 3, the amount of active power curtailed from all the PV units installed in the system is reduced, as can be observed in Fig. 4.

As expected, the RPC scheme is not totally efficient in mitigating the overvoltage problem in the system under study. In Fig. 5, there is a reduction in the voltage when RPC is employed, which is further enhanced with the combined operation of EN and DHN. The effectiveness of this combined control is justified by the reduction in the losses occurred in the EN. From the Table III it can be deduced that, using

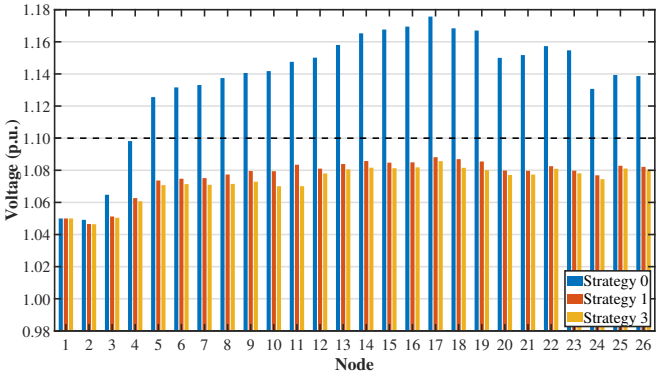

Fig. 3. Comparison of the node voltage corresponding to Strategy 0, Strategy 1 and Strategy 3.

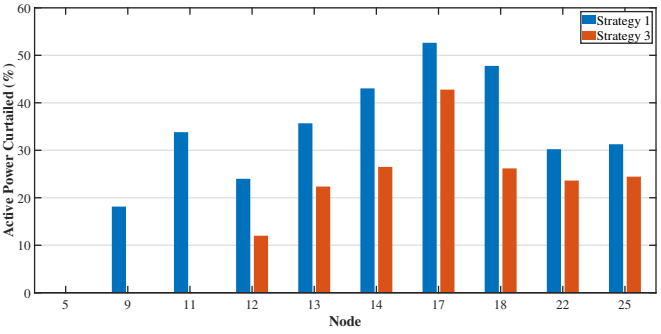

Fig. 4. Comparison of curtailed active power corresponding to Strategy 1 and Strategy 3.

Strategy 4, there is a loss reduction of 45.32 % compared to Strategy 2.

Considering DHN, node temperature is presented in Fig. 6 for the combined EN and DHN operation. The results corresponding to both the supply and the return subsystems are provided, for Strategies 3 and 4. From the slack bus to the final node of the radial DHN tested, the temperature is expected to decrease due to the thermal losses in the pipes of the supply subsystem. However, the HPs connected to the Nodes 3 and 5 affect the temperature profile; thus, an increase is noted in Node 5 due to the thermal power provided by the HP to the supply subsystem. Accordingly, in the return subsystem, the temperature drop is observed on the opposite direction, as the starting point here is the final node of the radial DHN, i.e., Node 7. The temperature in Nodes 4 and 2 in the return subsystem is also increased compared to the one in the previous nodes, which is observed because of the HPs installed in Nodes 5 and 3, respectively. Regarding the mass flow in the pipes, the results from the combined EN and DHN operation are presented in Table IV.

To better estimate the performance of the combined EN and DHN operation, a sensitivity analysis is performed by varying the rated power of the HPs installed, from 0.75 p.u. to 1.25 p.u.. In Fig. 7, the voltage in Node 17 is shown, for all the strategies. Node 17 is the node where the maximum voltage is observed when no strategy is applied (Strategy 0). It can be seen that increasing the installed capacity of the HPs, the node voltage is reduced for Strategies 3 and 4. Except for the decreased voltage, increasing the capacity of the HPs can also lead to less PV active power curtailment, as can be seen in Table V. Regarding network losses, a reduction is observed both in the EN and in the DHN, as shown in

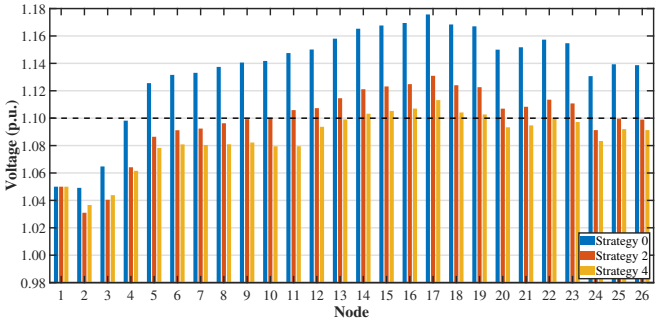

Fig. 5. Comparison of the node voltage corresponding to Strategy 0, Strategy 2 and Strategy 4.

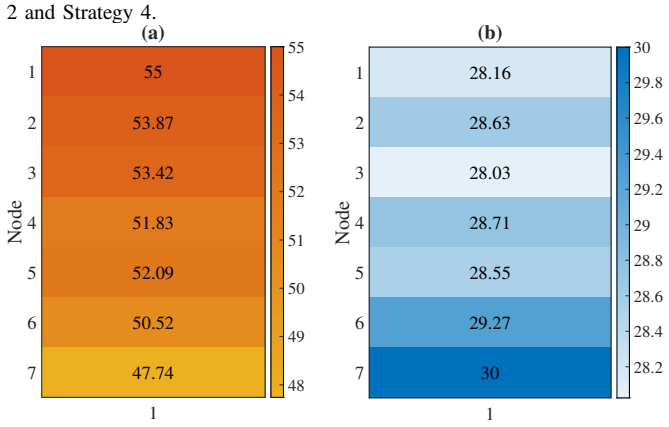

Fig. 6. Temperature in °C corresponding to the (a) supply subsystem and (b) return subsystem.

TABLE IV
MASS FLOW (KG/S) WITHIN EACH PIPE OF THE DHN FOR DIFFERENT VALUES OF THE HP THERMAL POWER (P.U.)

HP Thermal Power	Pipe 1-2	Pipe 2-3	Pipe 3-4	Pipe 4-5	Pipe 5-6	Pipe 6-7
0.75	0.96	0.57	0.88	0.45	0.76	0.41
0.80	0.92	0.52	0.86	0.42	0.76	0.41
0.9	0.84	0.44	0.81	0.38	0.76	0.41
1.00	**0.75**	**0.35**	**0.77**	**0.33**	**0.75**	**0.40**
1.10	0.67	0.26	0.72	0.28	0.75	0.40
1.20	0.58	0.18	0.68	0.23	0.74	0.39
1.25	0.54	0.13	0.65	0.21	0.74	0.39

TABLE V
ACTIVE POWER CURTAILMENT (%) IN NODE 17 WITH THE INCREASE IN THE HPS THERMAL POWER (P.U.)

0.75	0.80	0.90	1.00	1.10	1.20	1.25
45.58	45.10	43.98	42.76	41.57	40.36	39.76

TABLE VI
THERMAL LOSSES FOR DIFFERENT VALUES OF THE HP THERMAL POWER

HP Thermal Power		Thermal Losses
kW_{th}	%	kW_{th}
35.25	75	38.4831
37.60	80	38.4595
42.30	90	38.4048
47.00	**100**	**38.3356**
51.70	110	38.2415
56.40	120	38.0943
58.75	125	37.9745

Fig. 8 and Table VI, respectively. Finally, the installation of distributed thermal sources in a DHN results in local power provision to the thermal loads, which influences directly the mass flow values. Clearly, there is a reduction in the mass flow in the pipes, as observed in Table IV, a fact strongly related to the reduced thermal losses.

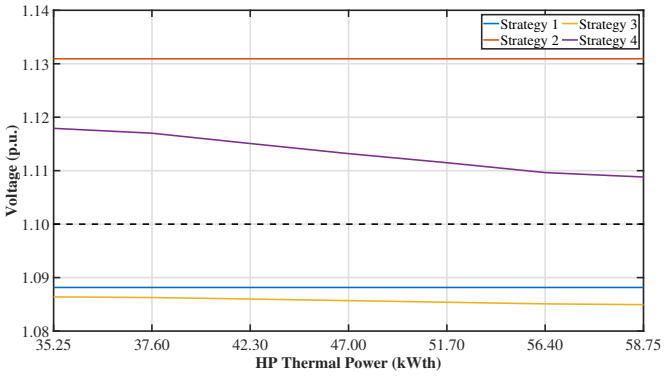

Fig. 7. Comparison of the voltage at Node 17 after applying all proposed control Strategies.

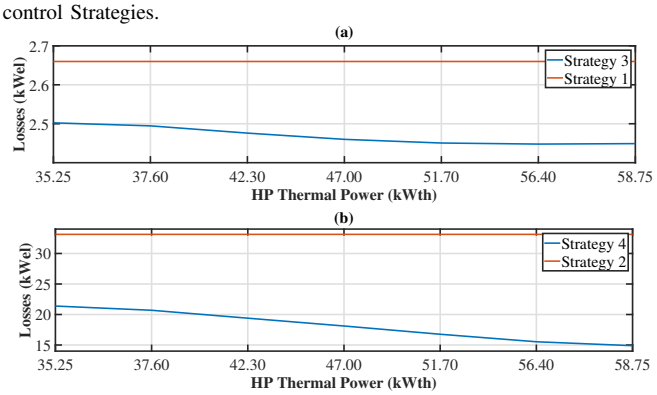

Fig. 8. Losses in the EN for the different values of the HPs thermal power. (a) Strategy 1 and Strategy 3 and (b) Strategy 2 and Strategy 4.

VI. CONCLUSIONS

In this paper, the integrated operation of EN and DHN is proposed to mitigate overvoltages in a LV EN with high PV penetration. At the same time, the well-established active and reactive droop control schemes for DRESs are applied and their effectiveness is evaluated regarding the voltage, the electrical and thermal losses and the exploitation of the active power generated by the DRES. Among the examined control strategies, Strategy 3, i.e., the APC scheme in collaboration with the combined operation of the two networks, seems to be the most efficient one both for mitigating overvoltages and reducing grid losses in the EN. Thus, the electrification of the thermal needs is a promising solution towards the better exploitation of the DRES potential, contributing at the same time to the elimination of the operational issues due to their high penetration into the existing ENs.

REFERENCES

[1] "Directive (EU) 2018/2001 of the European parliament and of the Council of 11 December 2018 on the promotion of the use of energy from renewable sources," Brussels, Tech. Rep. PE/48/2018/REV/1, 2018.

[2] R. Tonkoski, D. Turcotte, and T. H. M. El-Fouly, "Impact of high PV penetration on voltage profiles in residential neighborhoods," *IEEE Trans. Sustain. Energy*, vol. 3, no. 3, pp. 518–527, Jul. 2012.

[3] Voltage Characteristics of Electricity Supplied by Public Distribution Networks, BS EN Standard 50160, 2010.

[4] G. C. Kryonidis, E. O. Kontis, A. I. Chrysochos, C. S. Demoulias, and G. K. Papagiannis, "A coordinated droop control strategy for overvoltage mitigation in active distribution networks," *IEEE Trans. Smart Grid*, vol. 9, no. 5, pp. 5260–5270, Sep. 2018.

[5] Y. Wang, T. Zhao, C. Ju, Y. Xu, and P. Wang, "Two-level distributed volt/var control using aggregated PV inverters in distribution networks," *IEEE Trans. Power Del.*, vol. 35, no. 4, pp. 1844–1855, 2020.

[6] X. Li, W.Li, R. Zhang, et al., "Collaborative scheduling and flexibility assessment of integrated electricity and district heating systems utilizing thermal inertia of district heating network and aggregated buildings," *Applied Energy*, vol. 258, 2020.
[7] P. Mancarella, "MES (multi-energy systems): An overview of concepts and evaluation models," Energy, vol. 65, no.no. 2, pp. 1–17, 2014.
[8] R. Bacher, E. Peirano, M. Nigris, et al., "Vision 2050, Integrating Smart Networks for the Energy Transition: Serving Society and Protecting the Environment," Plan Innovate Engage, 2019
[9] "Powering a climate-neutral economy: An EU Strategy for Energy System Integration," Brussels, 8.7.2020, COM(2020) 299 final.
[10] Y. Jiang, C. Wan, A. Botterud, Y. Song and S. Xia, "Exploiting Flexibility of District Heating Networks in Combined Heat and Power Dispatch," *IEEE Trans. Sustain. Energy*, vol. 11, no. 4, pp. 2174-2188, Oct. 2020.
[11] C. Bernath, G. Deac, F. Sensfuß, "Impact of sector coupling on the market value of renewable energies – A model-based scenario analysis," *Applied Energy*, vol. 281, 2021.
[12] D. Meha, A. Pfeifer, N. Duić, H. Lund, "Increasing the integration of variable renewable energy in coal-based energy system using power to heat technologies: The case of Kosovo," *Energy*, vol. 212, 2020.
[13] Y. Zhou, M. Shahidehpour, Z. Wei, Z. Li, G. Sun and S. Chen, "Distributionally Robust Unit Commitment in Coordinated Electricity and District Heating Networks," *IEEE Trans. Power Syst.*, vol. 35, no. 3, pp. 2155-2166, May 2020.
[14] E. Widl, T. Jacobs, D. Schwabeneder, et al., "Studying the potential of multi-carrier energy distribution grids: A holistic approach," *Energy*, vol. 153, pp. 519–529, 2018.
[15] M. Aunedi, A. M. Pantaleo, K. Kuriyan, et al., "Modelling of national and local interactions between heat and electricity networks in low-carbon energy systems," *Applied Energy*, vol 276, 2020.
[16] S. Lu, W. Gu, K. Meng and Z. Dong, "Economic Dispatch of Integrated Energy Systems With Robust Thermal Comfort Management," IEEE Trans. Sustain. Energy, vol. 12, no. 1, pp. 222–233, Jan. 2021.
[17] M. Khatibi, J. D. Bendtsen, J. Stoustrup and T. Mølbak, "Exploiting Power-to-Heat Assets in District Heating Networks to Regulate Electric Power Network," *IEEE Trans. Smart Grid*, vol. 12, no. 3, pp. 2048–2059, May 2021.
[18] E. Widl, L.Benedikt, D. Basciotti, et al., "Combined Optimal Design and Control of Hybrid Thermal-Electrical Distribution Grids Using Co-Simulation," *Energies*, vol. 13(8), 2020.
[19] P. Yu, C. Wan, Y. Song and Y. Jiang, "Distributed Control of Multi-Energy Storage Systems for Voltage Regulation in Distribution Networks: A Back-and-Forth Communication Framework," *IEEE Trans. Smart Grid*, vol. 12, no. 3, pp. 1964–1977, May 2021.
[20] X. Liu, J. Wu, N. Jenkins, A. Bagdanavicius, "Combined analysis of electricity and heat networks," *Applied Energy*, vol. 162, pp. 1238–1250, 2016.
[21] Y. Chen, Y. Zhang, J. Wang, and Z. Lu, "Optimal Operation for Integrated Electricity–Heat System with Improved Heat Pump and Storage Model to Enhance Local Energy Utilization," *Energies*, vol. 13(24), 2020.
[22] S. Huang, W. Tang, Q. Wu and C. Li, "Network constrained economic dispatch of integrated heat and electricity systems through mixed integer conic programming," *Energy*, vol. 179, pp. 464–474,2019.
[23] R. Tonkoski and L. A. C. Lopes, "Voltage Regulation in Radial Distribution Feeders with High Penetration of Photovoltaic," 2008 IEEE Energy 2030 Conference, pp. 1–7, 2008.
[24] M. Taylor, S. Long, O. Marjanovic and A. Parisio, "Model Predictive Control of Smart Districts With Fifth Generation Heating and Cooling Networks," *IEEE Trans. Energy Convers.*, vol. 36, no. 4, pp. 2659-2669, Dec. 2021.
[25] Carrier, 30 RB/30RQV 040R-160R - Product selection data
[26] MATLAB 2018b, The MathWorks, Inc., Natick, Massachusetts, United States, 2018.